

COMPARISON OF FIVE NATURAL GAS EQUATIONS OF STATE USED FOR FLOW AND ENERGY MEASUREMENT

Aaron Johnson
NIST
100 Bureau Drive, Gaithersburg, MD
Aaron.Johnson@nist.gov

Bill Johansen
CEESI
54043 County Road 37, Nunn, CO,
BJohansen@ceesi.com

ABSTRACT

Measurements of the flow and the energy content of natural gas rely on equations of state to compute various thermodynamic properties including: 1) compressibility factor; 2) critical flow factor; 3) speed of sound; and 4) isentropic exponent. We compare these computed properties using five equations of state (REFPROP 8, GERG-2004, AGA 8, AGA 10, REFPROP 7) for eight natural gas compositions. The molar compositions vary from 97 % methane to 80 % methane; the latter has high levels of ethane, nitrogen, or carbon dioxide. These comparisons span the pressure and temperature ranges 0.1 MPa to 10 MPa and 270 K to 330 K. The five equations of state predict mutually consistent properties at low pressures. However, at higher pressures and lower temperatures inconsistencies among the speeds of sound are nearly 0.2 % and inconsistencies among critical flow factors are nearly 0.5 % for ethane-rich natural gas mixtures. For these mixtures the inconsistencies in the speed of sound are close to the AGA 9 limit of 0.2 %, and could influence ultrasonic flowmeter diagnostic capabilities that depend on accurate speed of sound predictions. In addition, the inconsistencies in the predicted values of the critical flow factor, if not resolved, could significantly reduce the accuracy of critical flow venturis when used in ethane-rich gases over select ranges of pressures and temperatures. The discontinuities discovered in the AGA 10 critical flow factors were as large as 0.075 %, and raise concerns about using this equation of state for critical flow venturi applications.

1. INTRODUCTION

The measurement of the flow and energy content of high pressure natural gas requires accurate thermodynamic properties. To meet this need numerous researchers have developed high accuracy equations of state for a wide range of natural gas mixtures. These equations are widely used in the flowmetering community both for custody transfer applications and for metering input/output along pipeline transmission networks. Consistency between these models is important to reduce measurement biases within the natural gas flowmetering community.

In this work we compare five commonly used equations of state including: 1) REFPROP 8 [1]; 2) GERG-2004 [2]; 3) AGA 8 [3]; 4) REFPROP 7 [4]; and AGA 10 [5]. These five equations of state are compared for each of the eight gases in Table 1¹ over the pressure range from 0.1 MPa to 10 MPa and at the three temperatures 270 K, 293.15 K, and 330 K. The thermodynamic properties that are compared include the compressibility factor (Z); the speed of sound (a); the critical flow factor (C^*); and the isentropic exponent (κ). These properties are routinely used in reducing data from commonly used natural gas flowmeters (e.g., ultrasonic flowmeters, turbine meters, critical flow venturis, and orifice flowmeters).

The American Gas Association has published several standards to document the accepted procedures and performance levels of various flowmeter types (e.g., ultrasonic flowmeters, turbine meters, orifice meters) used for measuring natural gas. In some cases, these standards require that thermodynamic properties associated with the flow measurement be made using a particular equation of state. For example, the AGA report number 9 [6] requires that the property calculations associated with ultrasonic flowmeters be made using AGA 10 (or methods that produce the same numerical results).

We show that NIST's REFPROP 8 in its AGA 8 mode produces values of Z , a , and κ ; identical to AGA 10. The values of C^* calculated with AGA 10 have problems. In particular, values of C_{AGA10}^* as a function of pressure along isotherms have discontinuities as large as 0.075 %. Moreover, the values of C_{AGA10}^* differed from the more accurate $C_{GERG-2004}^*$ equation of state by almost 0.5 % for ethane-rich natural gases. This difference is significant considering the number of flowmeter calibration laboratories (e.g., NIST, SwRI², CEESI³, WEPP⁴) that use critical flow venturis as working standards to calibrate other flowmeters. If these differences are not resolved, accurate CFV flow

¹The gas composition of *CEESI Colorado High Ethane* has an ethane concentration (10.6707 %) which exceeds the maximum limit (10 %) of the normal range in AGA 8.

²Southwest Research Institute (SwRI)

³Colorado Engineering Experimental Station Inc. (CEESI)

⁴China's West-East Pipeline Project (WEPP)

measurements may be infeasible for certain natural gas compositions at high pressures and low temperatures. In contrast, the maximum difference among predicted C^* values was less than 0.031 %

for methane rich gases with low levels of higher hydrocarbons.

Table 1. Eight Natural Gas Compositions¹

Component	Component Mole Fraction Percent for Indicated Gases							
	Gulf Coast	Amarillo	Ekofisk	High N ₂	High N ₂ /CO ₂	CEESI Iowa	CEESI Colorado High Ethane	CEESI Iowa High Ethane
Methane	96.5222	90.6724	85.9063	81.441	81.212	95.4850	84.8128	92.1244
Ethane	1.8186	4.5279	8.4919	3.3	4.303	1.8984	10.6707	4.3547
Propane	0.4596	0.828	2.3015	0.605	0.895	0.1770	1.7673	0.9299
Hydrogen	0	0	0	0	0	0.1599	0	0.1427
Nitrogen	0.2595	3.1284	1.0068	13.465	5.702	1.5987	0.409	1.1733
Carbon Dioxide	0.5956	0.4676	1.4954	0.985	7.585	0.5995	2.1109	0.9663
i-Butane	0.0977	0.1037	0.3486	0.1	0.151	0.0154	0.08	0.093
n-Butane	0.1007	0.1563	0.3506	0.104	0.152	0.02013	0.1258	0.1218
i-Pentane	0.0473	0.0321	0.0509	0	0	0.005	0.0115	0.0259
n-Pentane	0.0324	0.0443	0.048	0	0	0.003	0.01	0.024
Helium	0	0	0	0	0	0.03497	0	0.0293
n-Hexane	0.0664	0.0393	0	0	0	0.003	0.002	0.0147

2. BACKGROUND ON NATURAL GAS THERMODYNAMIC EQUATIONS OF STATE

NIST develops and maintains its own thermodynamic database named REFPROP. The latest version, REFPROP 8, was developed in 2007 to replace the 2002 version, REFPROP 7. REFPROP 8 includes three equations of state for natural gas mixtures:

- 1) the AGA 8 detailed characterization method originally developed in 1992 [3],
- 2) the standard GERG-2004 model [2], and
- 3) NIST's implementation of the GERG-2004 model.

The NIST implementation of the GERG-2004 uses higher accuracy equations for the pure gas components. This improvement makes the NIST version of the GERG-2004 equation of state more accurate than the standard version. Additionally,

REFPROP 8 includes the *complete version* of the AGA 8 equation of state.

The AGA 8 equation of state was developed in 1992 to calculate the compressibility factor for a wide range of natural gas mixtures at typical pipeline conditions [3]. The researchers who developed AGA 8 built in the capability to calculate sound speed and other thermodynamic properties in addition to the compressibility factor. However, only the results for the compressibility factor were published in the American Gas Association Report Number 8 [3]. At the time, many in the natural gas industry were ignorant that the complete AGA 8 equation of state could calculate all of the gas phase thermodynamic properties. Unaware of this capability the American Gas Association duplicated already existing capabilities when it developed AGA 10 in 2003 [5].

The AGA 10 equation of state is derived using the AGA 8 compressibility factor and the ideal gas

isobaric heat capacity [7]. The complete version of AGA 8 in REFPROP 8 uses the same expressions for the ideal gas isobaric heat capacity. Consequently, the thermodynamic properties in AGA 10 should be equivalent to those in REFPROP 8's implementation of AGA 8. With the exception of discontinuous C_{AGA10}^* values, the results herein verify this assertion.

Throughout this document the three REFPROP 8 models, the REFPROP 7 model, and the AGA 10 model are abbreviated using acronyms in Table 2.

Table 2. Abbreviated names and descriptions of the five equations of state are compared in this document.

Abbreviation for Equation of State	Brief Description of Each Equation of State
R8	NIST's version of the GERG-2004 equation of state in REFPROP 8 (Pure fluid equations are more accurate than standard GERG-2004)
R8-GERG	Standard GERG-2004 equation of state available in REFPROP 8
R8-AGA8	NIST's version of AGA 8 detailed characterization method available in REFPROP 8
AGA 10	Extension of AGA 8 equation of state by American Gas Association to enable additional properties to be calculated in addition to the compressibility factor
R7	the REFPROP 7 equation of state

Table 3. Uncertainty specifications for the five equations of state in the homogenous gas phase as claimed in the references.

Equation of State	Uncertainty of Compressibility Factor (Z)	Uncertainty of Speed of Sound (a)
R7	-	-
R8-AGA8	0.1 % [3]	0.2 % [2]
AGA 10	0.1 % [3]	0.1 % [5]
R8-GERG	0.1 % [2]	0.1 % [2]
R8	≤ GERG	≤ GERG

Table 3 shows the maximum expected uncertainty for the compressibility factor and sound speed for each of the equations of state over a wide range of compositions, pressures, and temperatures.⁵ Over a narrower range of conditions and gas compositions, lower uncertainties can be realized as demonstrated by numerous experimental data [2]. Although two of five equations of state (*i.e.*, AGA 10 and R8-GERG) have the same 0.1 % uncertainty in Z and a , the R8-GERG (or GERG-2004) is generally considered more accurate based on the following evidences [2]:

- 1) better agreement with experimental data at lower temperatures ($T < 275$ K)
- 2) better agreement with experimental data at higher pressures ($P > 10$ MPa), and
- 3) better agreement with experimental data for a wider range of gas compositions (such as gas mixtures with high ethane, nitrogen, and carbon dioxide)

In fact, the R8-AGA8 sound speed calculations have been assessed to have an uncertainty of 0.2 % - double that of the equivalent AGA 10 equation of state. The R8 equation of state is assumed to have a slightly lower uncertainty than the GERG-2004 model since its equations for the pure fluids comprising the natural gas mixture are more accurate. For this reason, R8 is taken to be the baseline when comparing the various equations of state in later sections.

3. RESULTS

In all cases the five equations of state agree within the uncertainty limits given in Table 3. As expected, the five equations of state agree best at higher temperatures and at lower pressures where virial effects are less significant. At higher temperatures the molecular kinetic energy is larger so that the molecular velocity (on average) is larger. The faster moving molecules are less affected by the intermolecular forces responsible for virial effects. Likewise, at low pressures the gas molecules are generally spaced further apart (*i.e.*, larger mean free path) so that intermolecular forces are less significant. These pressure and temperature trends are exhibited in the

⁵Consult the references in Table 3 for the full range of compositions, pressures, and temperatures that the uncertainty limits are applicable.

comparison data of the five equations of state in Sections 3.1, 3.2, and 3.3. In particular, for all of the compared properties the differences between the equations of state decrease at higher temperatures and tend toward zero at lower pressures.

No comparison data is presented for the isentropic exponent (κ). The maximum difference for κ between the five equations of state is only 0.42 %. This small difference has no significant impact on any of the flowmeters used for high pressure natural gas flows. For example, the expansion factor⁶ (which is used to account for compressibility effects in orifice meters) is affected by less than 0.037 % - an insignificant fraction of the total uncertainty of an orifice plate flow measurement.

3.1. Compressibility Factor (Z) Comparison Results

The compressibility factor (Z) is of the utmost importance in applications involving the flow and energy measurement of natural gases. Many of the flowmeters used to meter natural gas (*e.g.*, turbine meters, positive displacement meters, and ultrasonic flowmeters) measure volumetric flow. However, mass flow is often required. The compressibility factor is used to determine the density, which in turn, is used to convert from volumetric flow to mass flow (or equivalently volumetric flow at specified reference conditions). In addition, Z is important for calculating several other thermodynamic quantities including the heat capacity, enthalpy, entropy, speed of sound, and chemical potential. Figures 1, 2, and 3 show the percent difference of the compressibility factor for the five thermodynamic models at three temperatures $T = 270$ K, $T = 293.15$ K, and $T = 330$ K, respectively.

In Figs. 1 through 3 the Z values of the five equations of state generally agreed to better than 0.05 %. Differences larger than 0.05 % occurred for select gas compositions with the R7, R8-AGA8, and AGA 10 equations of state.

The R7 equation of state equation showed differences larger than 0.05 % for the Ekofisk and

CEESI Colorado High Ethane gas mixtures (*i.e.*, two gases with ethane concentrations above 8 %) and for High N_2/CO_2 (*i.e.*, a gas with CO_2 concentration above 7 %). For High N_2/CO_2 gas at $T = 270$ K the difference was as large as 0.19 %. The differences for all of the problem gases decreased with increasing temperature so that at $T = 330$ K the differences were less than 0.05 %. The differences observed at the lower temperatures have been confirmed experimentally for gases rich in ethane and for gases rich in CO_2 [2].

The AGA 10 and R8-AGA8 equations of state agreed to better than 0.0001 % for all but one gas composition (*i.e.*, CEESI Colorado High Ethane gas), which differed by no more than 0.009 %. This difference is likely caused by the ethane concentration exceeding the normal limits specified in AGA 8 (see Table 1). Both AGA 10 and R8-AGA8 agreed with R8 to better than 0.05 % for all but the High N_2 gas composition at $T = 270$ K. In this case the difference was less than 0.075 %. Good agreement was also found between the R8-GERG and R8 which differed by no more than 0.018 % for all eight gases in Figs. 1 through 3. The good agreement between the four equations of state (*i.e.*, R8-AGA8, AGA 10, R8-GERG, and R8) has also been confirmed experimentally [2]. However, experimental results are in better agreement with R8-GERG rather than the R8-AGA8 (or AGA 10) equations of state, especially at lower temperatures and higher pressures.

For the CEESI Iowa gas composition all five equations of state agreed to better than 0.014 % over the entire pressure range and for all three temperatures. This good agreement is a consequence of the high methane concentration (approximately 95.6 %) and low amounts of heavy hydrocarbons (*i.e.*, hexane less than 0.01 %). The good agreement suggests that for this gas composition the uncertainty of the equations of state are significantly lower than the values given in Table 3.

Below we summarize how these results apply to natural gas flow measurement applications requiring the compressibility factor:

- 1) Using R7 at low temperatures for natural gases rich in ethane or rich in CO_2 introduces additional uncertainty.

⁶The expansion factor calculations are based on correlations in AGA 3 [8]

- 2) AGA 10 and R8-AGA8 are identical for Z calculations.
- 3) The four equations of state (*i.e.*, AGA 10, R8-AGA8, R8-GERG, and R8) generally agree to better than 0.05 % for the eight gas compositions in Table 1 for $270 \text{ K} \leq T \leq 330 \text{ K}$ up to 10 MPa.
- 4) The CEESI lowa gas mixture (*i.e.*, more than 95 % methane and low amounts of heavy hydrocarbons) have compressibility factors that are easily characterized by existing equations of state, and are therefore ideal for flow measurement applications requiring density determination.

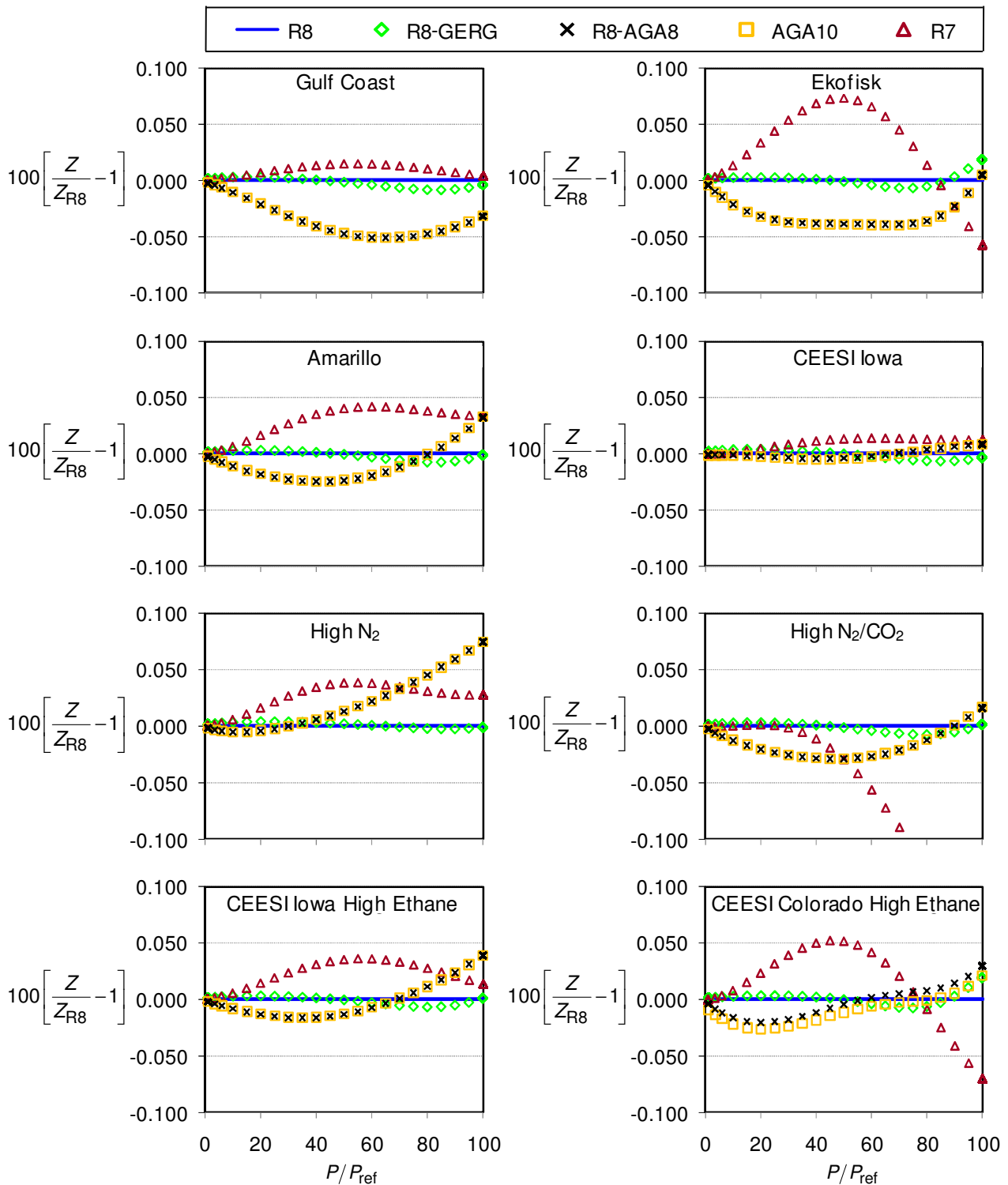


Figure 1. Percent difference between the compressibility factor (Z) of five thermodynamic models with R8 at $T = 270$ K where $P_{ref} = 101.325$ kPa.

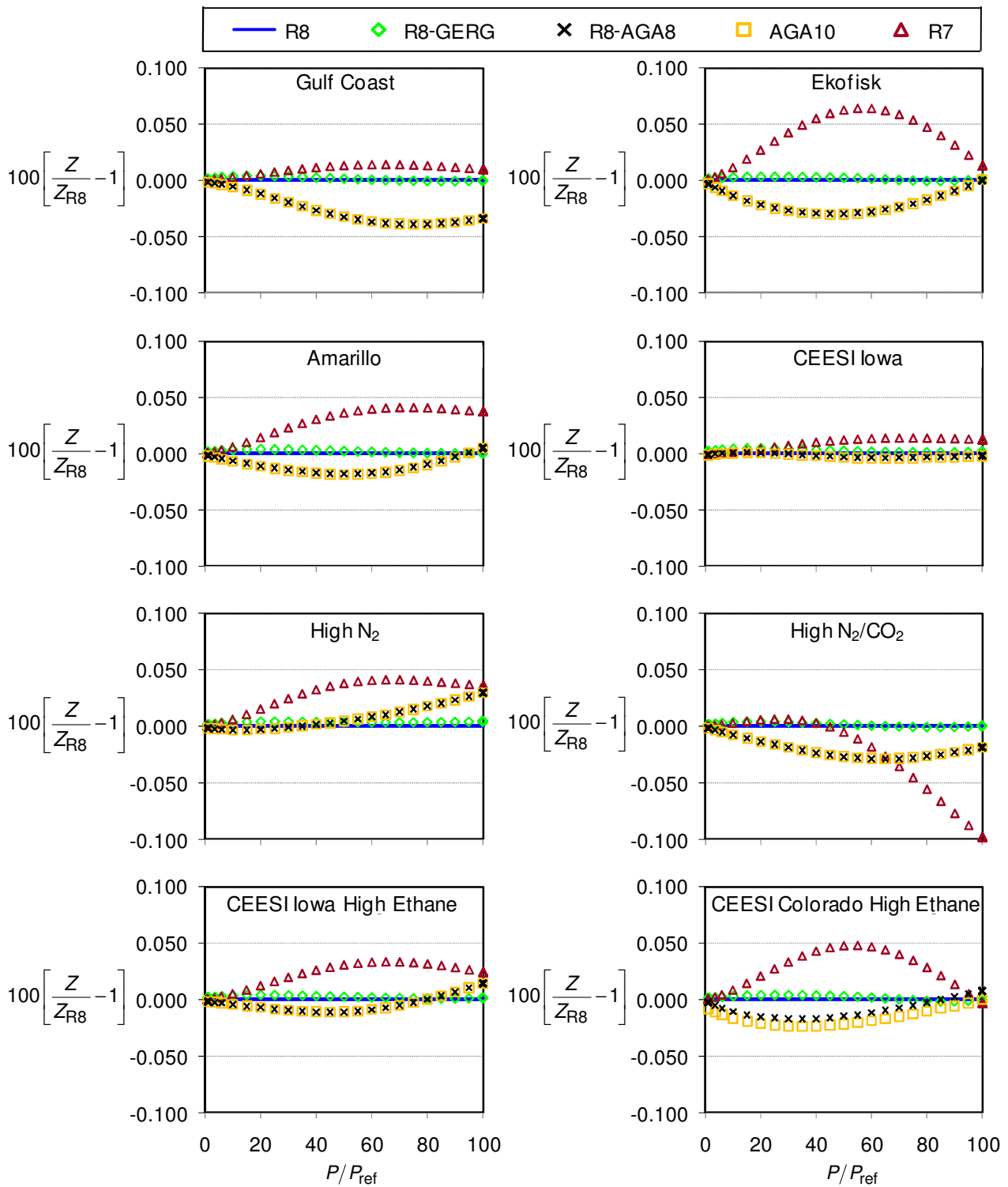


Figure 2. Percent difference between the compressibility factor (Z) of five thermodynamic models with R8 at $T = 293.15$ K and $P_{ref} = 101.325$ kPa.

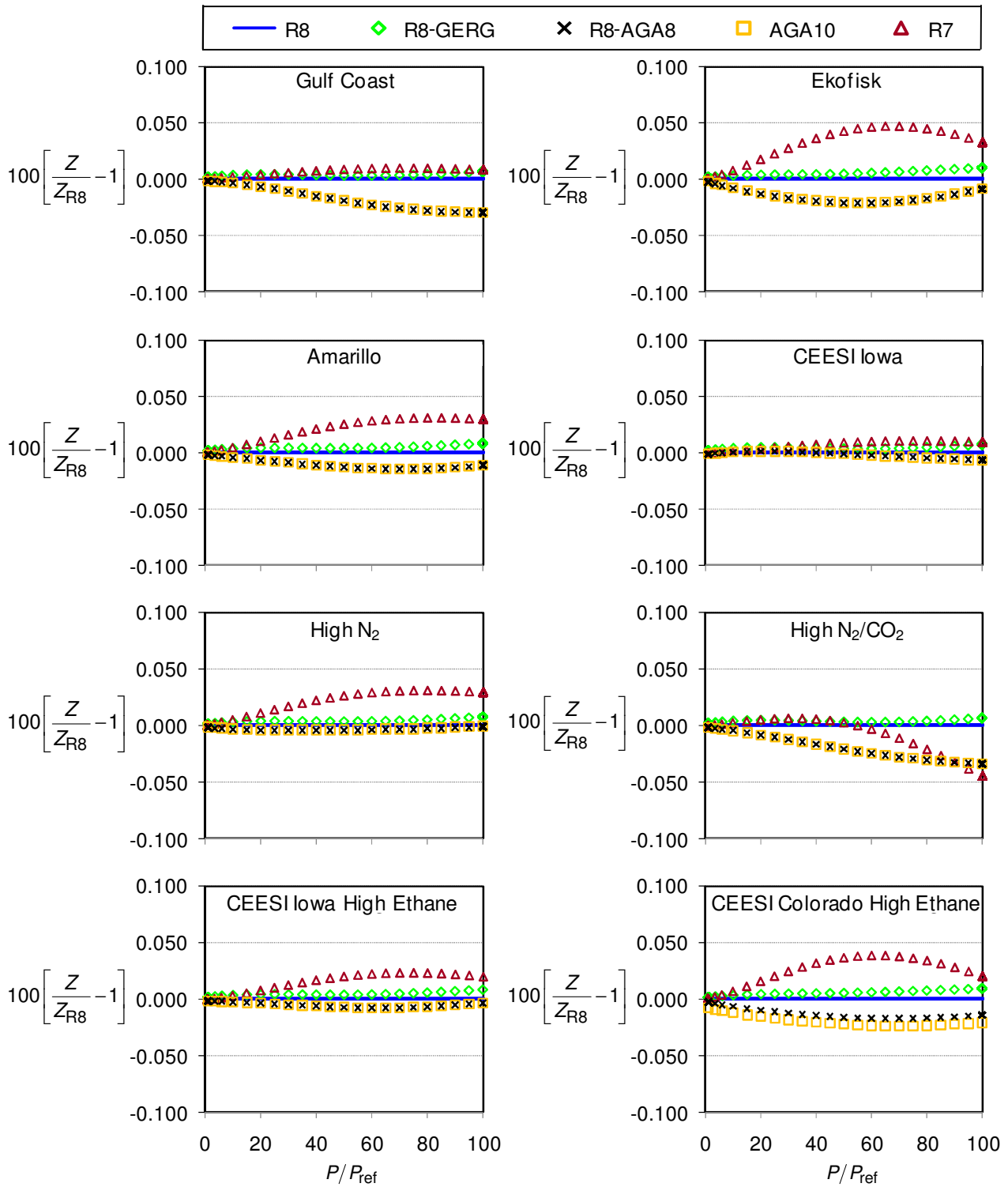


Figure 3. Percent difference between the compressibility factor (Z) of five thermodynamic models with R8 at $T = 330$ K and $P_{ref} = 101.325$ kPa.

3.2. Speed of Sound (a) Comparison Results

Multipath inline ultrasonic flowmeters are quickly becoming the industry standard for the custody transfer of dry pipeline quality natural gas. The flowmeter's popularity is a result of its good stability, high accuracy (after calibration), and numerous diagnostics. These diagnostics can help troubleshoot both the meter's performance as well as identify problems related to the flow/energy measurement process.

The flowmeter's ability to measure the speed of sound is the basis of several of its diagnostic capabilities. In practice, differences between the flowmeter reported speed of sound and the sound speed computed by a suitable equation of state can be used to identify problems with 1) the gas temperature measurement; 2) the gas pressure measurement; 3) the gas composition analysis; 4) the flowmeter's timing system; and/or 5) dimensional measurements of the transducer path lengths.

During a NIST flow calibration, the typical differences in the measured and calculated sound speeds are less than 0.1 %. During a zero flow verification test (*i.e.*, dry calibration), the maximum deviation compliant with AGA 9 is 0.2 %; however, most manufacturers design their meters to exceed these minimum expectations. If the threshold for the sound speed diagnostic is based on the level of agreement found during a flow calibration, then the uncertainty in the sound speed calculation should be 0.1 % or less. Furthermore, since the measurement conditions (*i.e.*, gas composition, pressure, and temperature) can differ significantly between the time when the flowmeter was calibrated in the laboratory and its use in the field, the calculated speed of sound must be independent of these parameters to levels better than 0.1 %.

Current industry practice is to calculate the speed of sound using AGA 10. For the ethane-rich gases in Fig. 4 (*i.e.*, Ekofisk and CEESI Colorado High Ethane) the AGA 10 sound speed (a_{AGA10}) deviates from the more accurate a_{R8} and $a_{R8-GERG}$ by more than 0.1 % at high pressures. Assuming that a_{R8} is correct, the error levels shown in Fig. 4 would trigger an alarm by the ultrasonic flowmeter sound speed diagnostic. However, in this case the cause of the alarm would be attributed to errors in

the equation of state, and not the flow/energy measurement process.

Problems with low temperature (*i.e.*, $T < 270$ K) sound speed calculations in AGA 10 have been documented by the measurements of Younglove [9] in reference [2] for gases rich in ethane. The problem is likely attributed to 1) the lack of low temperature (*i.e.*, $T < 270$ K) sound speed data during the formulation of the equation of state [2], and 2) a limited number of mixture compositions in the available sound speed data [10].

Analogous problems have been found for R7 at low temperatures. The High N_2/CO_2 gas at $T = 270$ K shown in Fig. 4 is one example of this problem. In this case the discrepancy between R7 and R8 is as large as 0.16 %. This difference persists even at the highest temperature of $T = 330$ K. The problems with the R7 speed of sound calculations are also discussed in reference 2 [2].

In general, Figs. 4 through 6 show if the low temperature ethane-rich gas compositions are excluded, a_{AGA10} agrees with both a_{R8} and $a_{R8-GERG}$ to better than 0.05 % for the majority of the gases over most (in some cases all) of the pressure range. Therefore, problems with AGA 10 sound speed calculations appear to be limited to low temperatures for select gas compositions. Finally, as expected, the AGA 10 and R8-AGA8 sound speed calculations are equivalent, $a_{AGA10} = a_{R8-AGA8}$.

The agreement between the $a_{R8-GERG}$ and a_{R8} is better than 0.01 % except at $T = 270$ K and $P/Pref > 80$ where differences can be as large as 0.05 %.

Below we summarize how these results apply to natural gas flow measurement applications requiring the speed of sound:

- 1) AGA 10 and R8-AGA8 are identical for sound speed calculations.
- 2) Either R8 or R8-GERG equations of state should be used for low temperature ($T < 270$ K) sound speed calculations at high pressures.

- 3) Calculation of the critical flow factor using R7, AGA 10 (or R8-AGA8) will likely incur larger uncertainties attributed to the need to calculate the sound speed at the CFV throat where the temperature will be significantly less than the stagnation temperature, T_0 .
- 4) Natural gas mixtures like the CEESI Iowa gas (more than 95 % methane) and low

amounts of heavy hydrocarbons have sound speeds that are easily characterized by existing models, thereby making this composition ideal for flow measurement applications involving ultrasonic flowmeters and CFVs.

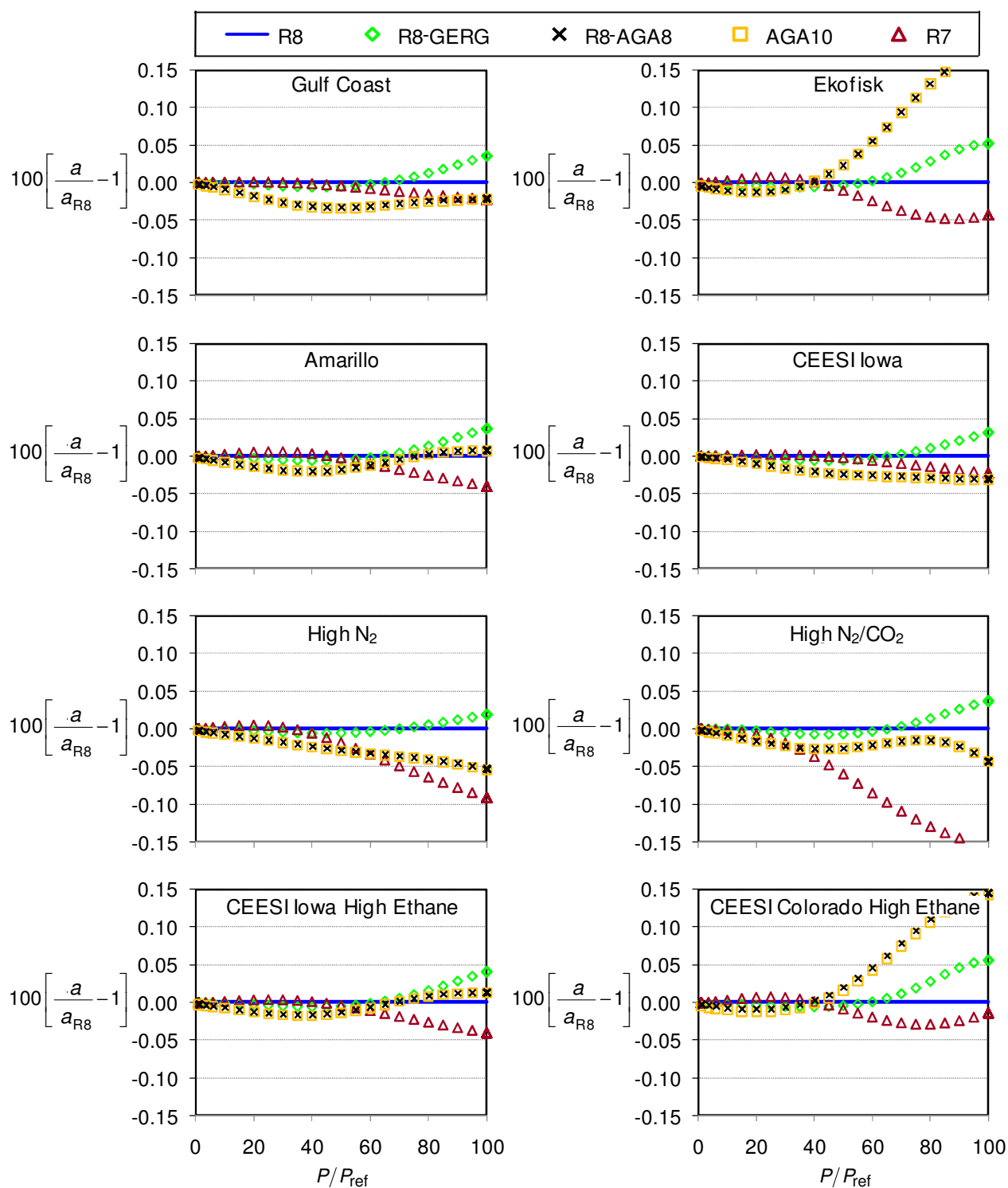


Figure 4. Percent difference between the speed of sound (a) of five thermodynamic models with R8 at $T = 270$ K where $P_{ref} = 101.325$ kPa.

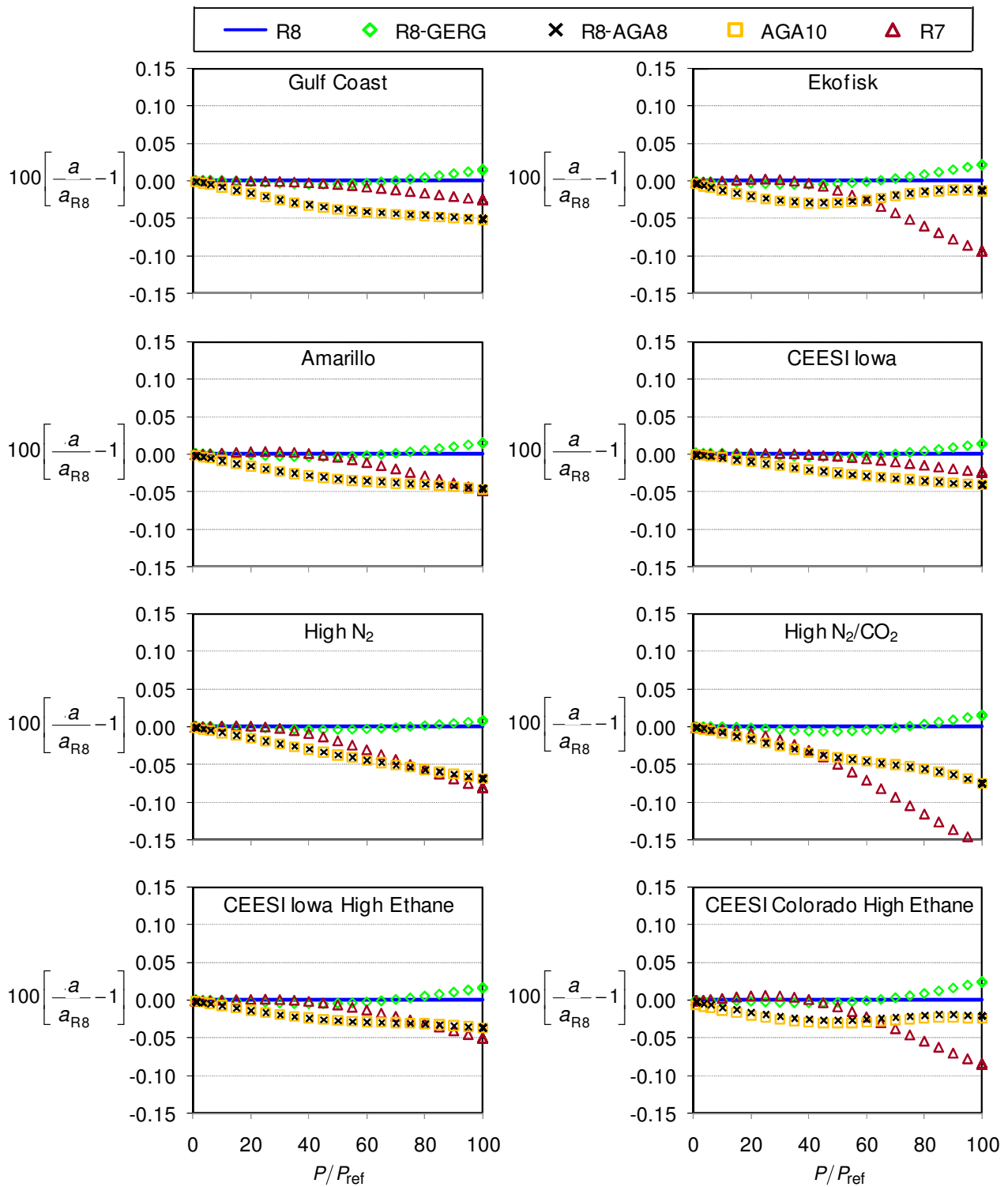


Figure 5. Percent difference between the speed of sound (a) of five thermodynamic models with R8 at $T = 293.15$ K where $P_{ref} = 101.325$ kPa.

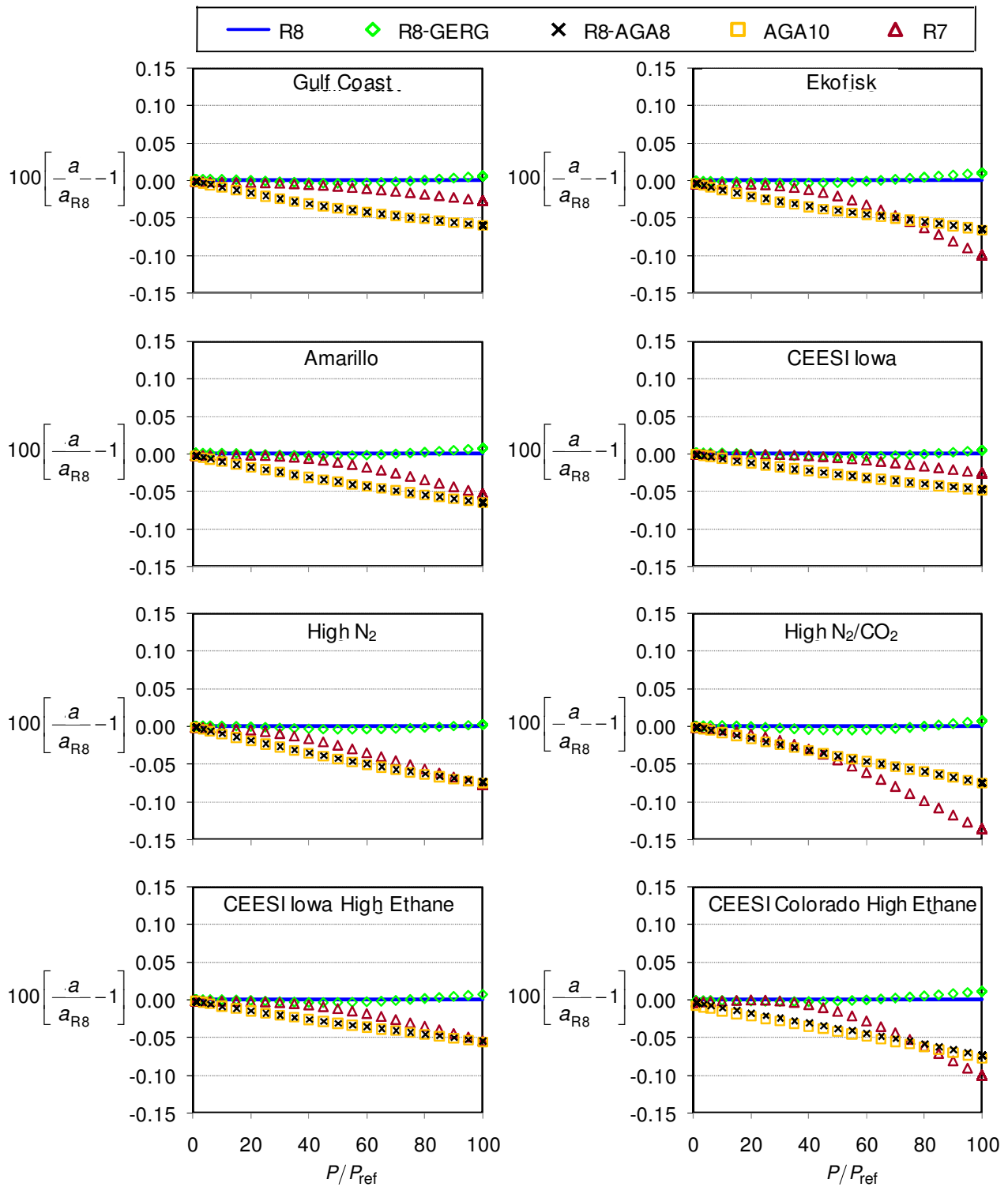


Figure 6. Percent difference between the speed of sound (a) of five thermodynamic models with R8 at $T = 330$ K where $P_{ref} = 101.325$ kPa.

3.3. Critical Flow Factor (C^*) Comparison Results

Critical flow venturis (CFVs) are widely used in the natural gas flowmetering community both as transfer standards [11] and as working standards [12, 13] to calibrate other flowmeters. Procedures detailing how CFVs are used in flow measurement applications are given in ISO 9300 [14]. Under choked flow conditions⁷ the CFV mass flow is

$$\dot{m} = \frac{C_d A^* C^* P_0 \sqrt{\mathcal{M}}}{\sqrt{R_u T_0}} \quad (1)$$

where P_0 is the stagnation pressure; T_0 is the stagnation temperature; C_d is the discharge coefficient determined by calibration; A^* is the throat cross sectional area; \mathcal{M} is the molar mass; R_u is the universal gas constant; and C^* is the critical flow factor.

The critical flow factor accounts for virial effects in CFV flows. When the fluid medium is a natural gas mixture at high pressure, virial effects are generally significant. In this case, accurate flow measurements rely heavily on the accuracy of the critical flow factor, as seen in Eqn. 1 where the flow is linearly dependent on C^* . Accurate C^* values, in turn, depend on the accuracy of the thermodynamic properties density and sound speed⁸, as seen in the definition of the critical flow factor [15]

$$C^* = \frac{\rho^* a^* \sqrt{R_u T_0}}{P_0 \sqrt{\mathcal{M}}} \quad (2)$$

where ρ^* and a^* are the density and speed of sound at the CFV throat (*i.e.*, minimum cross sectional area). Here, ρ^* and a^* are determined by simultaneously solving the following two equations [16]

$$h_0 = h^* + a^{*2}/2 \quad (3)$$

$$s_0 = s^* \quad (4)$$

⁷For choked flow conditions the pressure ratio (*i.e.*, downstream to upstream pressure) is below a critical threshold so that the flow velocity at the CFV throat equals the speed of sound.

⁸Accuracy also depends on accuracy of the equation of state to determine the entropy and enthalpy at the CFV throat and for stagnation conditions as shown in Eqns 3 and 4.

where h_0 and s_0 are the enthalpy and entropy evaluated at the stagnation conditions; and h^* and s^* are the enthalpy and entropy at the CFV throat. These equations relate the known stagnation conditions in the upstream piping of a CFV to the conditions at its throat. Thus, the throat conditions are not arbitrary, but are unique for a given gas composition and stagnation conditions.

To determine C^* Eqns. 3 and 4 are solved for ρ^* and a^* , which in turn are substituted into Eqn. 2. In general, Eqns. 3 and 4 must be solved numerically, using a suitable equation of state to evaluate the thermodynamic properties. Many thermodynamic packages (*e.g.*, AGA 10, R8, R8-GERG, R8-AGA8, *etc.*) have added C^* to the list of thermodynamic properties that can be calculated by the software. Thermodynamic packages with this capability typically calculate C^* based on user input values of P_0 , T_0 , and gas composition. For software packages not having this capability such as R7, the user must solve Eqns. 3 and 4 on their own.

In this work C^* values for R7 were computed in an Excel spreadsheet following the numerical method outlined in the Appendix. For the other four equations of state, C^* was calculated by the software package as a function of P_0 , T_0 , and gas composition. Figures 7 through 9 show the differences in C^* values calculated by the five equations of state. In all the figures the C^* values computed using the AGA 10 equation of state had discontinuities. In some cases the discontinuities were as large as 0.075 %. The y-axis scaling was decreased in Figs. 8 and 9 to clearly show the size of the discontinuities.

The R8-AGA8 equation of state (which in Sections 3.1 and 3.2 was shown to have identical compressibility factors, $Z_{R8,AGA} = Z_{AGA10}$, and sound speeds, $a_{R8,AGA} = a_{AGA10}$) did not exhibit any discontinuities. We therefore conjecture that the discontinuities in C^*_{AGA10} are related to the numerical method used to solve Eqns. 3 and 4. Probably a problem related to the convergence criteria.

Currently, there are no experimental measurements of C^* to compare to the predictions made by the various equations of state. Since discrepancies in the C^* predictions

cannot be rectified by comparison with data, one should 1) use equations of state with the lowest possible uncertainty budgets for sound speed and density, and 2) avoid using CFVs in (if possible) gas compositions, temperatures, and pressures where equally valid thermodynamic models disagree. Using this approach we would avoid the poor performance of the R8-AGA8 equation of state for Ekofisk natural gas in Fig. 7 based on the problems we identified with computing the sound speed in Fig. 4. On the other hand, gas compositions for which all the equations of state agree (such as the CEESI Iowa gas) are ideal for low uncertainty CFV applications.

In CFV applications the gas at the throat cross section will be significantly cooler than the upstream stagnation temperature attributed to the conversion of sensible energy into directed kinetic energy (or velocity). For example, for methane gas at upstream stagnation conditions of 10 MPa and 293.15 K, the throat temperature will be 248.06 K. Consequently, C^* should be calculated using equations of state (*e.g.*, R8 or R8-GERG) that give the highest accuracy of density and sound speed at low temperatures and high pressures.

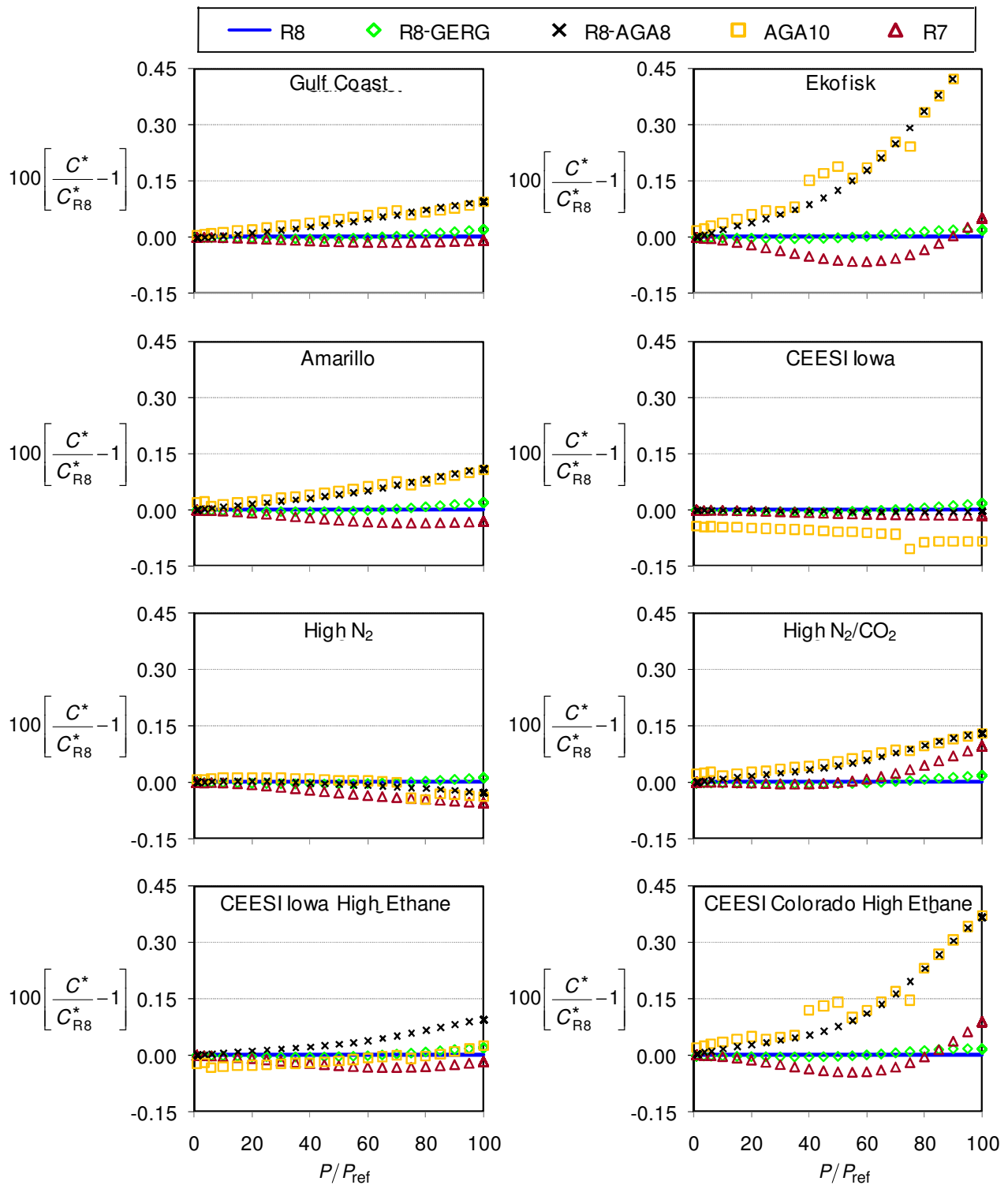


Figure 7. Percent difference between the critical flow factor (C^*) of five thermodynamic models with R8 at $T = 270$ K where $P_{ref} = 101.325$ kPa.

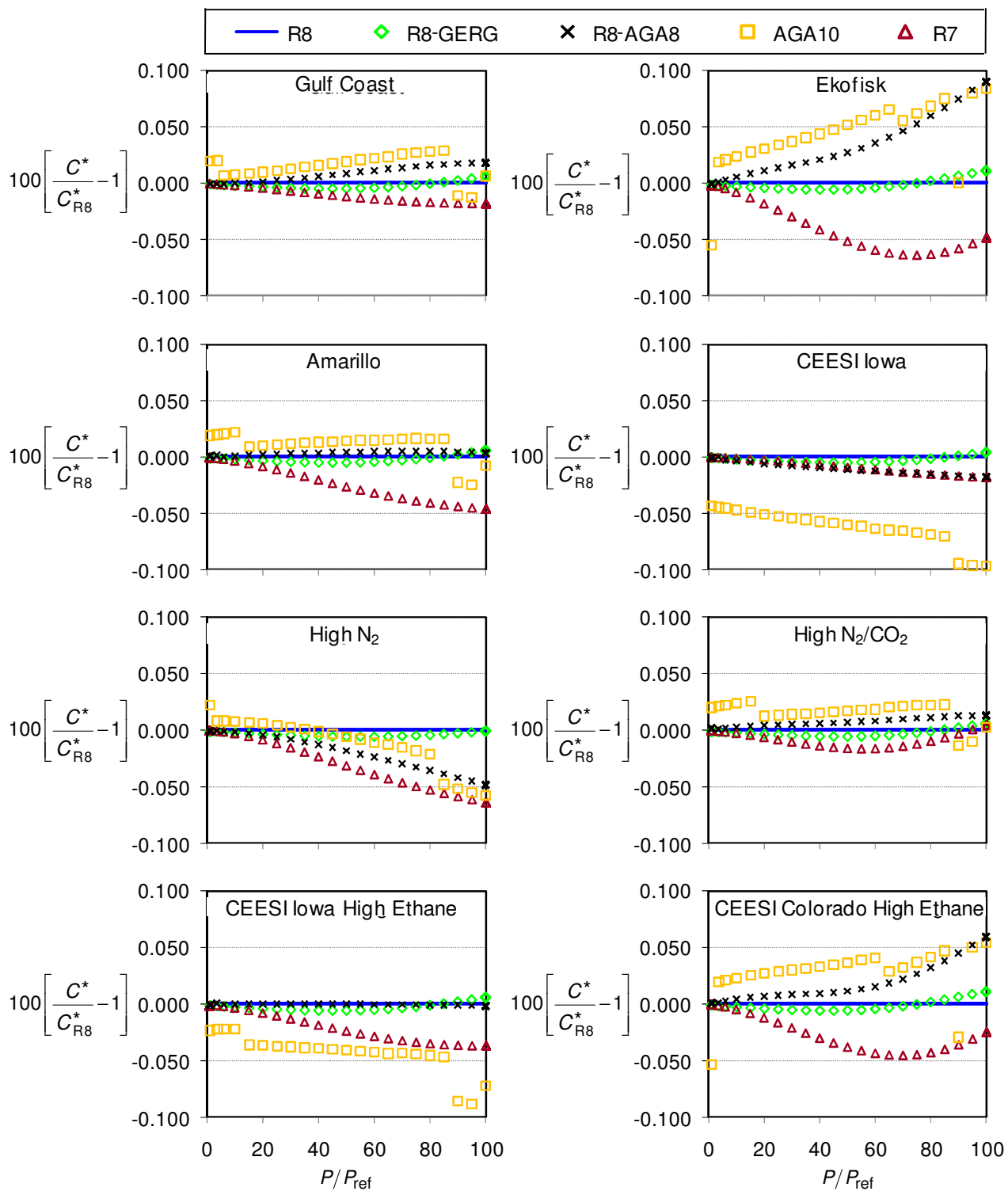


Figure 8. Percent difference between the critical flow factor (C^*) of five thermodynamic models with R8 at $T = 293.15$ K where $P_{ref} = 101.325$ kPa.

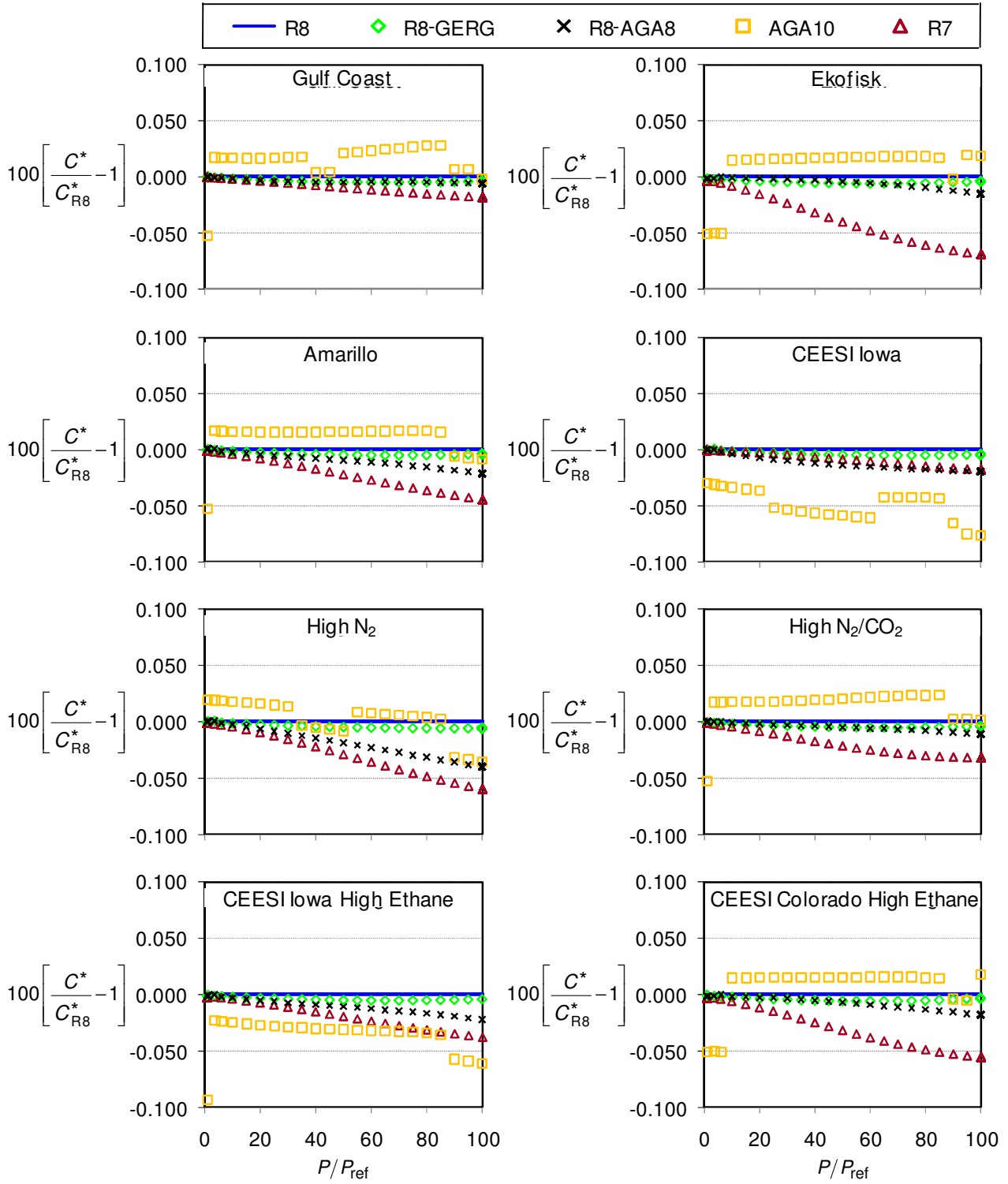


Figure 9. Percent difference between the critical flow factor (C^*) of five thermodynamic models with R8 at $T = 330$ K where $P_{ref} = 101.325$ kPa.

4. SUMMARY AND CONCLUSIONS

This work compared five equations of state commonly used in the natural gas flowmetering industry. The manuscript addressed how biases between these models could adversely affect flow measurement of various flowmeter types. In particular, we considered the compressibility factor, sound speed, critical flow factor, and isentropic exponent for eight gas types at pressures up to 10 MPa and at temperatures between 270 K and 330 K.

Biases in the isentropic exponent (which is used to calculate the expansion factor for orifice meters) were too small (i.e., less than 0.42 %) to impact orifice flow measurements.

The compressibility factor and sound speed were generally consistent between the five equations of state except at low temperatures for gas compositions rich in ethane or CO₂. The differences in the speed of sound were as large as 0.17 %. Biases of this level could negatively

impact the sound speed diagnostics associated with ultrasonic flowmeters. Worse yet, these biases could impair accurate calculation of the critical flow factor for CFV flowmetering applications.

The commonly used AGA 10 equations of state had unexplained discontinuities in its calculated critical flow factor as large as 0.075 %. For the other four equations of state, the differences in the critical flow factor varied from less than 0.031 % to almost 0.5 %, depending on gas composition, pressure, and temperature.¹⁷ The accuracy of CFVs depend on accurate values of the critical flow factor. At the present, no high accuracy measurements are available for the critical flow factor, and values must be obtained from thermodynamic equations of state. For gas compositions at conditions where large discrepancies exist between the best equations of state, the accuracy of CFVs are compromised.

REFERENCES

-
- [1] Lemmon, E. W., Huber, M. L., and McLinden, M. O. *NIST Standard Reference Database 23: Reference Fluid Thermodynamic and Transport Properties-REFPROP*, Version 8.0 National Institute of Standards and Technology, Standard Reference Data Program, Gaithersburg, 2007.
 - [2] Kunz, O., Klimeck, R., Wagner, W., and Jaeschke, M. *The GERG-2004 Wide-Range Equation of State for Natural Gases and Other Mixtures*, GERG TM15, 2007.
 - [3] Starling, K. E.; Savidge, J. L. *Compressibility factors of natural gas and other related hydrocarbon gases*, American Gas Association, Transmission Measurement Committee Report No. 8, Second Edition, 1992.
 - [4] Lemmon, E. W., McLinden, M. O., and Huber, M. L., *NIST Standard Reference Database 23: Reference Fluid Thermodynamic and Transport Properties-REFPROP Version 7.0* National Institute of Standards and Technology, Standard Reference Data Program, Gaithersburg, 2002.
 - [5] Transmission Measurement Committee, *AGA Report No. 10 Speed of Sound in Natural Gas and Other Related Hydrocarbon Gases*, American Gas Association, Washington, DC., 2003.
 - [6] Transmission Measurement Committee, *AGA Report No. 9, Measurement of Gas by Multipath Ultrasonic Meters*, American Gas Association, Washington, DC., 2007
 - [7] McFall, R.L., *Sonic nozzle flow calculation for natural gas using a generalized equation of state*, M.S. Thesis, University of Oklahoma, 1984.
 - [8] Transmission Measurement Committee, *Orifice Metering of Natural Gas Part 3: Natural Gas Applications*, AGA Report No. 3, 1992.
 - [9] Younglove, B. A.; Frederick, N. V.; McCarty, R. D., *Speed of sound data and related models for mixtures of natural gas constituents*. NIST, Monograph 178, Boulder, Colorado, 1993.

- [10] Savidge, J. L., *AGA10 Sound Speed Equations: Background, Thermodynamic Relations, Ideal Gas and Equation of State Methods, Uncertainty Analysis, and Calculation Flow Diagram for Natural Gas Measurement*, Fifth International Symposium on Fluid Flow Measurement, Washington, D.C., 2002.
- [11] Mickan, B., Kramer, R., Dopheide, D., Hotze, H., Hinze, H., Johnson, A, Wright, J., Vallet, J.-P., *Comparisons by PTB, NIST, and LNE-LADG, in Air and Natural Gas with Critical Venturi Nozzles Agree within 0.05 %*, Proceedings of the International Symposium on Fluid Flow Measurement, Queretaro, Mexico, 2006.
- [12] Johnson, A. N. and Kegel, T., *Uncertainty and Traceability for the CEESI Iowa Natural Gas Facility*, J. Res. Natl. Inst. Stand. Technol. 109, 345-369, 2004.
- [13] Johnson, A. N. and Johansen, B., *U.S. National Standards for High Pressure Natural Gas Flow Measurement*, Proc. of the 2008 Measurement Science Conference, Anaheim, CA (2008).
- [14] International Standards Organization, *Measurement of Gas Flow by Means of Critical Flow Venturi Nozzles*, ISO 9300:2005(E).
- [15] Johnson, R. C., *Calculations of Real-Gas Effects in Flow Through Critical Nozzles*, Journal of Basic Engineering, September 1964, pp. 519.
- [16] The American Society of Mechanical Engineers, *Measurement of Gas Flow by Means of Critical Flow Venturis, ASME/ANSI MFC-7M-1987*, 1987.
- [17] Press, W. H., Flannery, B. P. Teukolsky, S. A., Vetterling, W. T., *Numerical Recipes in Fortran*, Cambridge University Press, 1992. ISBN 0-521-43064-X (available online, with code samples)

APPENDIX

Critical Flow Factor Calculations

In general, Eqns. 3 and 4 must be solved iteratively using an accurate thermodynamic equation of state. The procedure suggested in the

ASME standard MFC-7M [15] gives a procedure for solving Eqns. 3 and 4 of Section 3.1 to determine the critical flow factor. However, the procedure was written more than 20 years ago, and implicitly assumed that the CFV user would calculate enthalpy, entropy, sound speed, etc. from the compressibility factor explicit in temperature and pressure in conjunction with the ideal gas heat capacity. Consequently, the procedure given was generic, and gave CFV end-users flexibility to select the appropriate numerical algorithms.

Unfortunately, many CFV users are not adept using numerical methods. Consequently, the flexibility built into the MFC-7M solution procedure has caused confusion, and has led to solution methods that are cumbersome to use, converge slowly, and occasionally give the wrong (or only partially converged) values of C^* . To provide guidance we herein outline a numerical procedure that can be used to compute C^* . The following method was implemented into an Excel spreadsheet to compute C^* values using the REFPROP 7 equation of state discussed in this work.

A Numerical Procedure to Compute C^*

- 1) Use the thermodynamic equation of state to compute $s_0 = s(T_0, P_0)$ and $h_0 = h(T_0, P_0)$ at the stagnation conditions T_0 , and P_0 . (For simplicity composition dependence is not shown.)
- 2) Define the throat enthalpy, $h^* = h(T^*, s^*)$, and the throat sound speed, $a^* = \sqrt{h(T^*, s^*)}$, as a function of the throat entropy, $s^* = s_0$, which is equal to the stagnation entropy (and is known from the stagnation conditions in step 1), and the unknown throat temperature, T^* , which must be determined.

Equation 3 and 4 are reduced to a single equation with T^* as the only unknown.

$$h_0 = h(T^*, s^*) + a^2(T^*, s^*)/2 \quad (5)$$

However, T^* must be solved numerically as it is an implicit function of both the enthalpy and the square of the sound speed.

- 3) Define a percent difference error function for the n^{th} iteration

$$\varepsilon_n = 100 \left[\frac{h(T_n^*, s^*) + a^2(T_n^*, s^*)/2}{h_0} - 1 \right] \quad (6)$$

equal to the percent difference between throat variables (*i.e.*, the throat enthalpy and kinetic energy) and the stagnation enthalpy. By definition, if $\varepsilon_n = 0$ then $T_n^* = T^*$ (*i.e.*, Eqn. 5 is satisfied so that the iterative procedure is converged).

- 4) Define an acceptable convergence tolerance (*e.g.*, tolerance = 0.000001)
- 5) Guess Initial Conditions:
 - a) Guess two throat temperatures: $T_1^* = 2T_0/\gamma + 1$ and $T_2^* = (T_1^* + T_0)/2$ (Note any reasonable choices for temperatures are adequate to start the iterative procedure.)
 - b) Calculate the values of the error function for the two guessed temperatures T_1^* and T_2^* using Eqn. 6. These values of the error function are taken to be the errors for the 1st and 2nd iterations, $\varepsilon_1 = \varepsilon(T_1^*)$ and $\varepsilon_2 = \varepsilon(T_2^*)$.
- 6) Use the Newton-Raphson Iteration method [17] to determine T_{n+1}^* for the next iteration.

$$T_{n+1}^* = T_n^* - \varepsilon_n \left/ \frac{d\varepsilon}{dT^*} \right|_n \quad (7)$$

where the derivative term is estimated numerically by

$$\left. \frac{d\varepsilon}{dT^*} \right|_n = \frac{\varepsilon_n - \varepsilon_{n-1}}{T_n^* - T_{n-1}^*} \quad (8)$$

- 7) Calculate the error function for the new temperature, T_{n+1}^* using Eqn. 6, $\varepsilon_{n+1} = \varepsilon(T_{n+1}^*)$.
- 8) Check to see if $|\varepsilon_{n+1}| < \text{tolerance}$. If yes, proceed to step 9, and if not return to step 6 and complete another iteration (*i.e.*, increase n by one).

- 9) The value of T_{n+1}^* determined from step 6 is the converged throat temperature (based on the selected tolerance). Use $T^* = T_{n+1}^*$ along with known throat entropy (s^*) to calculate the following:
 - a) the throat density, $\rho^* = \rho(T^*, s^*)$, and
 - b) the throat sound speed, $a^* = a(T^*, s^*)$.

- 10) Use Eqn. 2 to compute C^*